Autoimmune cardiomyopathy and heart block develop spontaneously in HLA-DQ8 transgenic IAβ knockout NOD mice

John F. Elliott[†‡], Junliang Liu[†§], Zuan-Ning Yuan[†¶], Norma Bautista-Lopez[†], Sarah L. Wallbank[†], Kunimasa Suzuki[†], David Rayner[∥], Patrick Nation[††], Murray A. Robertson[‡‡], Gang Liu[§§], and Katherine M. Kavanagh[§§]

Departments of [†]Medical Microbiology and Immunology and [∥]Laboratory Medicine and Pathology, [††]Health Sciences Laboratory, Animal Services, [‡‡]Pediatric Cardiology Division of Department of Pediatrics, and [§§]Cardiology Division of Department of Medicine, Faculty of Medicine and Dentistry, University of Alberta, Edmonton, AB, Canada T6G 2S2

A line of nonobese diabetic (NOD) mice expressing the human diabetes-associated HLA-DQ8 transgene in the absence of mouse IA$_β$ failed to show spontaneous insulitis or diabetes, but rather developed dilated cardiomyopathy, leading to early death from heart failure. Pathology in these animals results from an organ- and cell-specific autoimmune response against normal cardiomyoctes in the atrial and ventricular walls, as well as against very similar myocytes present in the outermost muscle layer surrounding the pulmonary veins. Progression of the autoimmune process could be followed by serial ECG measurements; irradiation of young animals significantly delayed disease progression, and this effect could be reversed by adoptive transfer of splenocytes taken from older animals with complete heart block. Disease progression could also be blocked by cyclosporin A treatment, but was accelerated by injection of complete Fruend's adjuvant. The constellation of findings of spontaneously arising destructive focal lymphocytic infiltrates within the myocardium, rising titers of circulating anticardiac autoantibodies, dilation of the cardiac chambers, and gradual progression to end-stage heart failure bears a striking resemblance to what is seen in humans with idiopathic dilated cardiomyopathy, a serious and often life-threatening medical condition. This transgenic strain provides a highly relevant animal model for human autoimmune myocarditis and postinflammatory dilated cardiomyopathy.

Idiopathic dilated cardiomyopathy (IDCM) describes a condition whereby previously healthy individuals develop life-threatening heart failure associated with enlargement of the heart, but with no apparent underlying cause (1, 2). The cardiac pathology seen in the majority of IDCM patients indicates a recent or more long-standing immune-mediated inflammatory process within the muscle tissue of the heart (i.e., myocarditis) (3, 4). IDCM patients often demonstrate circulating anticardiac autoantibodies, and the myocarditis is generally thought to arise from an autoimmune response against cardiac tissues (5). Research on IDCM has been hampered by the lack of an appropriate animal model, that is, a model where animals develop disease spontaneously, show severe life-threatening pathology, and display an immunological and histological picture similar to that seen in humans with IDCM.

The human MHC class II molecule DQ8 (i.e., haplotype DQA1*0301, DQB1*0302) is known to be associated with type 1 diabetes (T1D). To map DQ8-restricted T cell epitopes for T1D autoantigens we crossed DQ8 transgenic nonobese diabetic (NOD) mice with a NOD MHC class II β-chain knockout line (6). Because the resulting animals express the human MHC class II molecule but not the mouse, any CD4$^+$ T cells arising would be restricted to the human MHC molecule. We chose the NOD strain because it is known to have defects in self-tolerance, which we hypothesized would aid our efforts to induce immune responses against self-antigens such as GAD65. Although replacement of the murine T1D-associated class II MHC molecule with

the closely related human DQ8 molecule might have been expected to preserve the autoimmune diabetes phenotype, we found that the anti-β cell responses were replaced with anticardiomyocyte responses once the IA^{g7} was removed. This article characterizes the heart disease seen in these animals and demonstrates that the pathology is mediated by cells of the immune system.

Materials and Methods

Mice and Disease Monitoring. The origins of the $DQ8^{+/+},IA_β^{-/-}$ NOD mice (also called human CD4, DQA1*0301, DQB1*0302 transgenic IAnull NOD) have been described (6).

Histology and Immunohistochemistry. Fresh biopsies were fixed in formalin and paraffin sections stained with hematoxylin and eosin; half of each tissue was used to make frozen sections, which were immunostained for CD4 and CD8 T cells. Immunostaining for B lymphocytes used rehydrated paraffin sections.

Echocardiography. High-quality 1D images with time in the horizontal axis (M-mode) were obtained in the parasternal short and long views at the papillary muscle level, using real-time directed imaging.

ECG. Nonsedated mice were placed in an appropriate-sized syringe barrel with portions cut out to allow access to the feet. Separate electrodes were clipped to the four foot pads, and ECG leads I, II, III, AVR, and AVL were simultaneously recorded.

ELISA and T Cell Proliferation Assays. Sera were collected from $DQ8^{+/+},IA_β^{-/-}$ NOD animals at various ages and from control strains at 20 weeks of age. Porcine cardiac myosin (Sigma M0531) was used to establish a direct ELISA using standard methods. Methods used to measure T cell proliferative responses have been described (6).

Irradiation, Adoptive Transfer, Cyclosporin A (CsA), and Complete Freund's Adjuvant (CFA) Treatments. For the adoptive transfer experiments 5-week-old $DQ8^{+/+},IA_β^{-/-}$ NOD mice were irradiated (850 rads) with a 137Cs instrument (Gammacell 40, MDS Nordion, Ottawa). Serum and splenocytes (purified over lympholyte M gradients) were collected from transgenic animals ≥24 weeks of age that had shown complete atrioventricular

IMMUNOLOGY

(AV) block for at least 2 weeks. Fresh sera and splenocytes from several animals were pooled, and 200 μl of sera and/or 1×10^7 splenocytes was transferred by separate i.p. injections. In the CsA experiment animals received daily injections of CsA (10 mg/kg s.c.) or an equivalent volume of PBS from weaning until 15 weeks of age. For the CFA experiment 3-week-old mice received a single i.p. injection of 50 μl of CFA (Difco) emulsified with 50 μl of PBS. In all experiments animals were monitored by weekly ECG, and the age at which prolonged PR interval (≥ 35 msec) and/or complete AV block appeared was noted. PR interval is the time from the beginning of the P wave (which represents atrial contraction) to the beginning of the QRS complex (which represents ventricular contraction).

Additional Details. See *Supporting Text*, which is published as supporting information on the PNAS web site.

Results

Fatal Heart Failure Associated with Enlarged Hearts and Pancarditis.
Animals from the original DQ8 transgenic NOD line were found to develop spontaneous autoimmune diabetes at the same rate as the regular NOD/LtJ strain (i.e., 85–90% of females became diabetic by 32 weeks of age in both our NOD and $DQ8^{+/+}$ NOD in-house breeding colonies). However, when the DQ8-NOD animals were crossed with the NOD class II MHC knockout line, resulting $DQ8^{+/+},IA_\beta^{-/-}$ NOD animals no longer developed any diabetes or insulitis, but instead developed progressive dilated cardiomyopathy (hearts three to four times normal size; Fig. 1*A*) and heart failure leading to premature death in both males and females (Fig. 2*A*). The autopsy finding of cardiac enlargement was confirmed in preterminal animals >20 weeks of age by *in vivo* measurements using high-resolution M-mode echocardiography, which demonstrated significant enlargement and extremely poor contractile function of both ventricles (Fig. 2*B*).

Histological examination of end-stage hearts showed pancarditis, with grossly dilated atria (often with a large organized thrombus in the left atrium) and few live cardiomyocytes remaining in mostly fibrotic atrial walls, which in places were paper thin (Fig. 1*B*). Areas of the atrial wall where cardiomyocytes remained were invaded by mononuclear cells, and the associated muscle cells appeared to be dead or dying (Fig. 1*C*). In the ventricles, both endocardial and epicardial/perivascular regions showed scattered foci of infiltrating mononuclear cells, and these were invariably contacting areas of cardiomyocyte damage and loss (Fig. 1 *B*, *D*, and *E*). The mononuclear cells consisted primarily of B lymphocytes and plasma cells, with lesser numbers of CD4$^+$ and CD8$^+$ T cells (Fig. 1 *H–J*). Histological examination of all other tissues from preterminal animals failed to show any extra cardiac mononuclear cell infiltrates, except for very occasional foci in the skeletal muscles and the salivary glands of animals >30 weeks of age. In the DQ8$^{+/+}$ NOD line (i.e., $IA^{g7+/+}$, diabetes-susceptible) and the NOD $IA_\beta^{-/-}$ line (i.e., the two progenitor lines) we found no evidence of heart enlargement or myocarditis at any age.

Earliest Mononuclear Cell Infiltrates Occur Around Pulmonary Veins.
In contrast to the older preterminal animals, 5-week-old $DQ8^{+/+}$, IA_β knockout animals showed minimal or no mononuclear cell infiltrates within the heart; when present, these were confined to the atria, just at the base of the great vessels. However, when all of the other organs of these younger animals were carefully examined, marked lymphocytic infiltrates were found specifically in the lungs in every case. The infiltrates were localized exclusively to the outermost muscle layer that surrounds the pulmonary veins of rodents (Fig. 1*G*, compare with normal mouse pulmonary vein in Fig. 1*F*). This layer consists of striated muscle fibers known as ensheathing cardiomyocytes; these cells form a sphincter-like structure around the vein, express α-cardiac my-
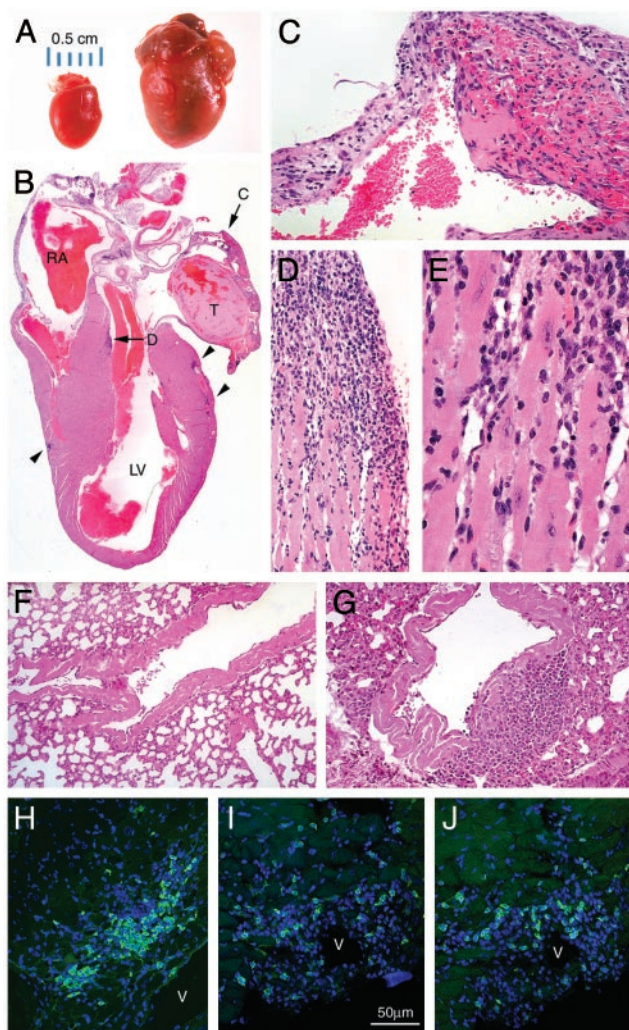
Fig. 1. (*A*) Photograph of intact heart from a 22-week-old preterminal $DQ8^{+/+},IA_\beta^{-/-}$ female NOD mouse (*Right*; 0.57 g) compared with that of a healthy age- and sex-matched NOD/LtJ animal (*Left*; 0.14 g). (*B–E*) Histology of a typical end-stage diseased heart, stained with hematoxylin and eosin (representative of $n = 12$ animals). (*B*) Areas indicated by arrows are shown at higher power in *C* and *D*. RA and LV indicate right atrium and left ventricle, respectively. A large organized thrombus (T) fills most of the left atrium. Atrial walls are extremely thin, and the muscle has been replaced with fibrous tissue in most places. Residual patches of dying atrial cardiomyocytes stain bright pink (*C*) and are associated with mononuclear cell infiltrates. Dense focal mononuclear cell infiltrates associated with myocyte damage can be seen in the ventricular endocardium (*D*; and at higher magnification in *E*) and in a perivascular location on the epicardial surface (*B*, arrowheads). The perivascular mononuclear cells were characterized further by indirect immunofluorescence. The majority of cells showed surface or cytoplasmic IgG expression consistent with B lymphocytes and plasma cells (*H*; light blue-green staining cells); smaller numbers of CD4$^+$ and CD8$^+$ T cells were also clearly present (*I* and *J*, respectively). V, epicardial blood vessel. Note that in *H–J* all cellular nuclei fluoresce dark blue because of 4′,6-diamidino-2-phenylindole counterstaining, and muscle proteins within the cardiomyocytes fluoresce dark green. *F* and *G* show, respectively, pulmonary veins from a normal 5-week-old NOD/LtJ and a 5-week-old $DQ8^{+/+},IA_\beta^{-/-}$ animal. (*G*) A dense collection of mononuclear cells is seen to be associated with the destruction of the ensheathing cardiomyocyte layer on the lower right aspect of the pulmonary vein. Note that during fixation the surrounding lung was less well inflated in *G* than in *F*. (Magnifications: *B*, ×3; *C* and *D* and *F–J*, ×100; *E*, ×400).

osin heavy chain, and beat spontaneously at 60 Hz (7). The foci of lung mononuclear cells contacted areas of ensheathing cardiomyocyte damage and loss (Fig. 1*G*). Reexamination of pul-
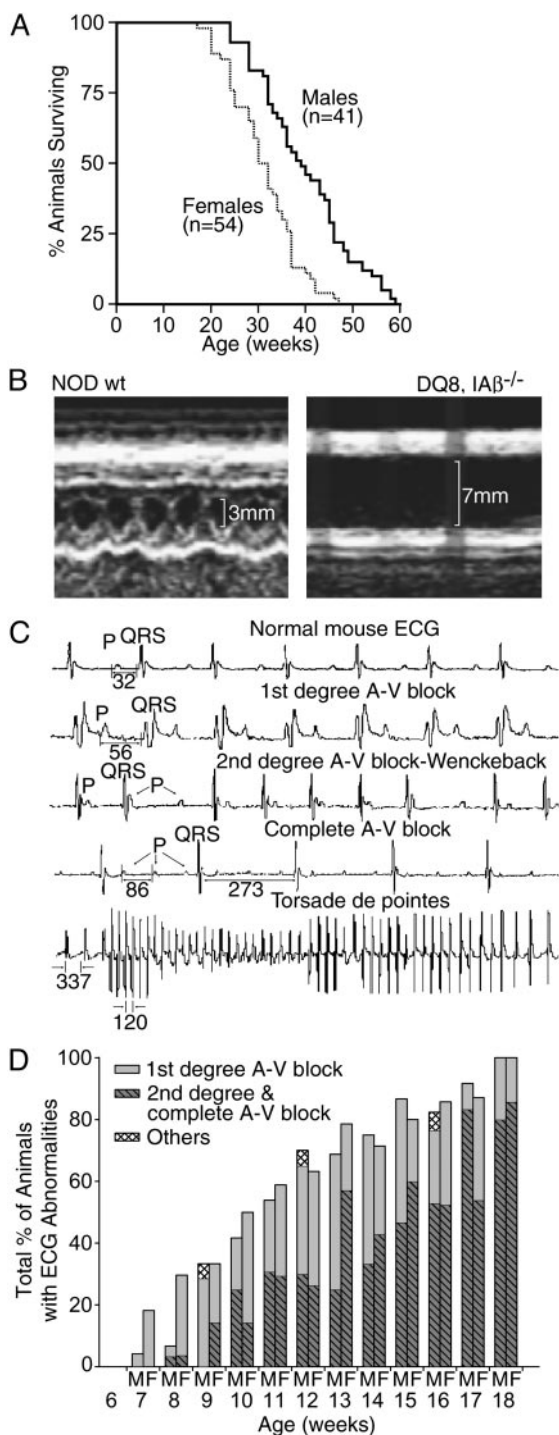
Fig. 2. (A) Survival curves for male and female $DQ8^{+/+},IA_\beta^{-/-}$ mice. Animals were monitored from 12 weeks of age onward; severely ill animals were killed. (B) M-mode echocardiogram from a healthy 20-week-old female NOD/Lt mouse (*Left*) versus a preterminal $DQ8^{+/+},IA_\beta^{-/-}$ NOD (*Right*). The location of the anterior and posterior endocarial walls is defined by the brackets, with time along the *y* axis. The NOD heart has a normal anteroposterior diameter and is seen to contract normally over time, whereas the diseased heart is significantly dilated and barely contracts (representative of *n* = 8 animals). Echocardiography also revealed other abnormalities such as mitrial regurgitation in older animals (data not shown). (C) Representative ECG traces taken from a normal mouse (NOD/LtJ; top trace) and $DQ8^{+/+},IA_\beta^{-/-}$ NOD animals of various ages (lower four traces). P waves and QRS complexes are indicated; numbers indicate lengths of various intervals in msec. Note that the time scale in the bottom trace differs from the rest. (D) Summary of ECG findings for male (M) and female (F) $DQ8^{+/+},IA_\beta^{-/-}$ NOD mice of various ages.

monary veins from older preterminal mice demonstrated that the ensheathing cardiomyocyte layer had completely disappeared in these animals, and because no mononuclear cell infiltrates remained in the lungs, this anatomical subtlety had not been noted when the sections were first examined. Lungs from animals of intermediate ages (e.g., 11 weeks) showed an intermediate pattern; that is, those regions of the pulmonary veins that were completely denuded of ensheathing cardiomyocytes were free of associated mononuclear cells, whereas adjacent regions where ensheathing cardiomyocytes remained showed mononuclear cell aggregates in direct contact with myocytes undergoing apparent damage and dropout. These and additional observations led us to conclude that the destructive immune-inflammatory process begins in the pulmonary vein ensheathing cardiomyocytes, and then gradually moves centrally to involve the (antigenically similar) atrial and ventricular cardiomyocytes. As the targeted muscle cells around the pulmonary veins are removed, the mononuclear infiltrates within the lung resolve in a manner similar to what is seen for a diabetic islet once all of the β cells have been destroyed.

Animals Develop Progressive Conduction Abnormalities (Heart Block) Detected by ECG. Serial ECGs were performed on a large number of $DQ8^{+/+},IA_\beta^{-/-}$ NOD animals at various ages to assess the effect of the myocarditis on the electrophysiological function of the heart. Fig. 2*C* shows representative traces, and Fig. 2*D* shows a compilation of our findings. These investigations showed that at 6 weeks of age virtually all animals had a normal ECG profile, essentially identical to that found in NOD/LtJ, which was taken as the control strain, whereas by 7 weeks some animals began to demonstrate first-degree AV block, indicating a delay in the conduction of the depolarizing signal that ordinarily moves through the atria (causing the P wave) and thence through the ventricles (causing the QRS complex). As the animals aged, the first-degree AV block became much more widespread in the population, and by 18 weeks the majority of animals had progressed to second degree or complete AV block, where transfer of the depolarizing signal from the atria to the ventricles is either intermittently or completely blocked (i.e., in the latter case the P waves and QRS complexes become dissociated, and the rate of ventricular depolarization slows to that dictated by an ectopic ventricular pacemaker; see Fig. 2*C*, fourth trace). In a minority of animals other more unusual ECG patterns were observed, such as Wenckeback and Torsade de pointes (Fig. 2*C*).

Increasing Titers of Anticardiac Autoantibodies and T Cell Responses Against Cardiac Myosin Arise Spontaneously. The histological picture of myocarditis seen in the $DQ8^{+/+},IA_\beta^{-/-}$ NOD animals (i.e., foci of mononuclear cells in contact with dead and dying cardiomyocytes) suggested that the disease process might be autoimmune in origin. We therefore investigated these animals for the presence of anticardiac autoantibodies and T cell responses. Direct immunofluorescence assay (IFA) failed to reveal any significant *in vivo* deposition of mouse autoantibodies on the surfaces of cells within the diseased heart tissues. However, when frozen sections of normal mouse heart were tested by indirect IFA using serum from >25-week-old animals with complete heart block, there was strong staining of both nuclei and cytoplasm within the cardiomyocytes (data not shown). Positive results with the indirect IFA were followed up with Western blots made from muscle proteins extracted from mouse atria or ventricles and mouse skeletal muscle (Fig. 3*A*). For comparison, commercially available porcine skeletal myosin and porcine cardiac myosin were included in the blot. Serum from a 6-week-old animal detected two different protein bands present in the mouse heart extracts (fine band at ≈150 kDa, thicker band at ≈190 kDa). An analogous pattern but slightly weaker signal was seen in the lane containing the purified porcine cardiac myosin,

IMMUNOLOGY
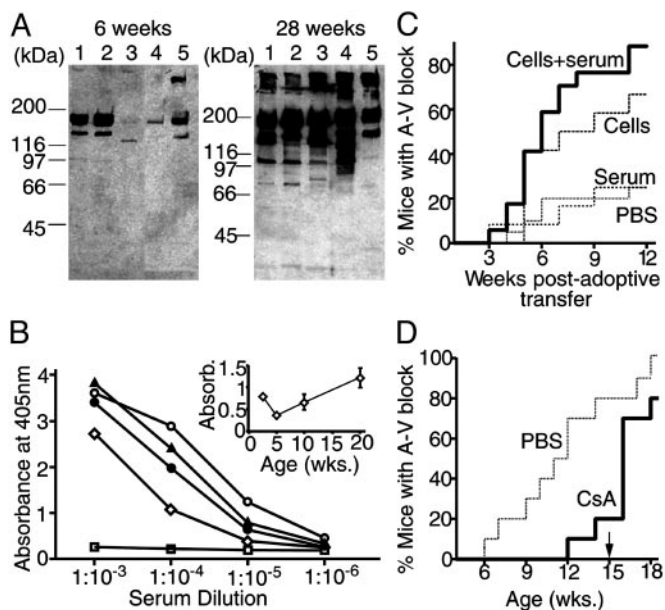
Fig. 3. (*A*) Identical Western blots made with heart muscle proteins and probed with sera from two different $DQ8^{+/+},IA_\beta^{-/-}$ NOD animals (*Left*, 6-week-old animal without heart block, 1:10,000 dilution; *Right*, 28-week-old animal with complete AV block, 1:50,000 dilution). Lanes contain muscle proteins extracted from: 1, mouse atria; 2, mouse ventricles; 3, mouse skeletal muscle or purchased commercially from Sigma; 4, purified porcine skeletal myosin; and 5, purified porcine cardiac myosin. (*B*) Titration curves for anticardiac myosin antibodies present in the sera of $DQ8^{+/+},IA_\beta^{-/-}$ NOD mice of various ages. Sera were pooled from animals ages 2.5 weeks ($n = 9$; ▲), 5 weeks ($n = 7$; ◇), 10 weeks ($n = 7$; ●), and 20 weeks ($n = 6$; ○). As a control, values for pooled sera from $DQ8^{+/+},IA_\beta^{g7+/+}$ NOD mice ($n = 5$; □) are also shown. A number of other control strains (NOD/Lt, $IA_\beta^{-/-}$ NOD, C57BL/6) were similarly negative. Total serum IgG concentrations in older preterminal $DQ8^{+/+},IA_\beta^{-/-}$ NOD animals were somewhat higher (up to 4-fold increased) compared with those found in control strains. ELISA plates were coated with porcine cardiac myosin, incubated with various dilutions of pooled antisera and then secondary antibodies, and developed with horseradish peroxidase. The data are expressed as mean of pooled sera tested in triplicate. (*Inset*) Data replotted as absorbance versus age for pooled sera at the 1:100,000 dilution. (*C*) Incidence of heart block in irradiated animals that received adoptive transfer of splenocytes, cells ($n = 12$), serum ($n = 12$), both agents ($n = 17$), or PBS only ($n = 20$). All animals were irradiated at 5 weeks of age, injected as indicated, and then followed with weekly ECGs. The percentage of animals showing first-degree or complete heart block at various weeks posttransfer are indicated. The serum and PBS groups were not statistically different, nor were the cells vs. cells plus serum groups. At 11 and 12 weeks, the cells group statistically differed from the PBS group with $P = 0.03$. Similarly, at 11 and 12 weeks, the cells plus serum group differed from the PBS group with $P = 0.001$. Fisher's exact test was used to calculate two-tailed P values. (*D*) Heart block in animals receiving CsA injections vs. PBS. Beginning at weaning, animals were given daily injections of CsA (10 mg/kg s.c) or PBS ($n = 10$ animals in each group). Values indicate the percentage of animals with first-degree or complete heart block. CsA injections were discontinued at 15 weeks of age (indicated by arrow). At 14 and 15 weeks, the two groups were statistically different ($P = 0.023$) by Fisher's exact test.

and much weaker signals still were detected in the lanes containing skeletal muscle proteins. Probing an identical Western blot with serum from a 28-week-old mouse gave a much stronger signal and detected additional bands; in particular, the antibodies present now clearly bound the ≈190-kDa band in the skeletal muscle extracts. This result and the histological finding of occasional skeletal myositis in older animals are consistent with the idea that over time there is epitope spreading and "immunological escalation" of the autoimmune response, which apparently generalizes from cardiac myocytes to also include skeletal myocytes and their antigens.

We used commercially available porcine cardiac myosin to establish a solid-phase ELISA to measure anticardiac myosin IgG autoantibody titres in pooled antisera from $DQ8^{+/+},IA_\beta^{-/-}$ NOD mice of various ages (Fig. 3*B*). Significant anticardiac myosin autoantibodies were detected at 3 weeks of age (likely transferred in the mothers' milk, based on our unpublished observations using cross-fostering), and these reached a minimum by 5 weeks of age and thereafter rose continually as the animals aged, reaching titers as high as $1:10^6$ by 20 weeks of age. These same antisera showed no ELISA reactivity to BSA or another commercially available cardiac antigen (porcine laminin), and they reacted very weakly to double-stranded DNA (highest titers 1:100). Sera from a variety of other mouse strains (WT NOD, DQ8 NOD, NOR, C57/BL6, and BALB/c) showed no reactivity to cardiac myosin in this ELISA.

Splenocytes from $DQ8^{+/+},IA_\beta^{-/-}$ NOD mice proliferated in the presence of porcine cardiac myosin (Table 1), and these responses could be blocked with an anti-DQ mAb, but not with an isotype-matched control antibody. A similar proliferative response was not elicited with equivalent concentrations of a control xeno-antigen (bovine B₂-microglobulin), and the acetylated myosin peptide Ac614–643 (8, 9) did not appear to cause significant T cell proliferation.

Heart Block and Myocarditis Could Be Adoptively Transferred. To establish that the immune system was playing a role in causing the heart block and myocarditis, we performed adoptive transfer experiments, transferring serum, splenocytes, or a mixture of the two into 5-week-old irradiated animals, and then following the animals for the onset of first degree or complete AV block (Fig. 3*C*). Irradiation of animals at 5 weeks of age reduced the incidence of AV block to ≈25% by 17 weeks of age (vs. expected levels of ≥80% for untreated animals, Fig. 2*D*), and postirradiation transfer of serum alone was no more effective than PBS at restoring the disease process. In contrast, postirradiation transfer of cells alone or cells plus serum induced AV block in a significant fraction of the irradiated animals (Fig. 3*C*). Interestingly, animals that received cells and serum appeared to develop the highest levels of heart block by 12 weeks posttransfer, although this group was not statistically different from the group that received cells only. At 13 weeks posttransfer all animals were killed, and their hearts were examined microscopically and scored blindly for the severity of myocarditis and atrial wall infiltrates with a graded scale of 0–5. Average histology scores for the various groups were as follows: PBS, 0.4 ± 0.1 ($n = 20$); serum, 0.5 ± 0.1 ($n = 12$); cells, 2.3 ± 0.2 ($n = 12$); and cells plus serum, 2.8 ± 0.3 ($n = 17$).

Treatment with CsA Delays Appearance of Heart Block, and CFA Precipitates It. In addition to irradiation, we tested the effect of other immune interventions on progression to AV block in the $DQ8^{+/+},IA_\beta^{-/-}$ NOD animals. Animals that received daily injections of CsA (10 mg/kg) from weaning onward showed a considerable delay in progression to AV block in comparison to a control group receiving daily injections of PBS (Fig. 3*D*). However, CsA treatment at this dose was unable to completely block disease progression (i.e., some animals in the CsA group began to show AV block by 12–14 weeks of age), and when the drug was discontinued at 15 weeks most of the animals in the treatment group rapidly developed AV block. Because a single injection of CFA at 4 weeks of age can delay or prevent the onset of autoimmune diabetes in WT NOD mice (10), we were interested to know what effect this immune intervention might have in our myocarditis model. Paradoxically, administration of CFA to 4-week-old $DQ8^{+/+},IA_\beta^{-/-}$ NOD mice precipitated complete AV block in all animals (10 of 10) by 12–13 weeks of age, regardless of whether or not the animals had first-degree AV block in the preceding week (i.e., more typically animals initially

Table 1. Proliferative responses of DQ8$^{+/+}$, IA$_\beta$$^{-/-}$ NOD splenocytes

Antigen	Concentration, μg/ml	Blocking agent	cpm ± SEM	Stimulation index
Exp. 1				
Medium only	—	—	905 ± 219	1.00
+Cardiac myosin	12.5	—	2,029 ± 361	2.24
+Cardiac myosin	50	—	2,799 ± 653	3.09
+Bovine B$_2$ microglobulin	12.5	—	1,005 ± 213	1.11
+Bovine B$_2$ microglobulin	50	—	884 ± 303	0.98
Exp. 2				
Medium only	—	—	1,547 ± 5.5	1.00
+Cardiac myosin	25	—	3,210 ± 329	2.07
+Cardiac myosin	25	Anti-DQ McAb	1,394 ± 273	0.90
+Cardiac myosin	25	Isotype control	2,990 ± 174	1.93
+Myosin Ac614–643	25	—	1,697 ± 120	1.10

For additional details see *Supporting Text*.

develop first-degree AV block and then progress to complete block). This finding may relate to the capacity of lipopolysaccharide and other adjuvants to increase MHC class II expression on heart interstitial cells (11).

Additional Results. For additional details see *Supporting Text*.

Discussion

A number of mouse models of autoimmune myocarditis have been characterized in the past. Mice of the A background were shown by Rose and colleagues (12) to be susceptible to both post-Coxsackie virus B3 and myosin-induced experimental autoimmune myocarditis, and Penninger's group (8) described myosin-induced autoimmune myocarditis in the BALB/c strain. Bachmeier *et al.* (13) showed that HLA-DQ6 transgenic mice were also susceptible to autoimmune myocarditis after immunization with cardiac myosin. All of these models, however, require either prior infection with Coxsackie virus or deliberate immunization with cardiac myosin in adjuvant. Mouse models of spontaneous autoimmune myocarditis and dilated cardiomyopathy have also been created by using two different approaches: (*i*) transgene-mediated cardiomyocyte-specific overexpression of tumor necrosis factor α (TNF-α) (14–16), and (*ii*) crossing a PD-1 receptor knockout line onto the BALB/c background (17). The TNF-α transgenic animals developed severe transmural myocarditis; between the various founder lines severity of disease was proportional to levels of expression of the proinflammatory cytokine. In contrast to the DQ8 NOD model described here, the PD-1 receptor knockout BALB/c animals showed no apparent infiltration of mononuclear cells within the myocardium. Rather, histology showed only sporadic interstitial fibrosis with scar formation. All affected animals developed high-titer circulating IgG autoantibodies, which reacted with an unidentified 33-kDa protein expressed specifically on the surface of cardiomyocytes. Direct immunofluorescence analysis revealed linear deposits of IgG and complement on the surface of cardiomyocytes, suggesting an antibody-mediated disease process (17). This is very different from the typical picture of clinical myocarditis seen in humans, where foci of mononuclear cell infiltrates and focal cardiomyocyte destruction are observed. Thus the $DQ8^{+/+},IA_\beta^{-/-}$ NOD model not only develops spontaneous disease, but presents a histological and immunological picture much closer to what is seen in humans (18).

The DQ8 transgenic line described here was created directly in the NOD background. Descriptions of at least two other DQ8 transgenic, IAb knockout mouse lines (and their derivatives) have been published by David and colleagues (19–21) and Wen and colleagues (22–24); those lines have been used to investigate a number of autoimmune models, particularly type 1 diabetes.

Yet neither line has been reported to develop spontaneous autoimmune myocarditis. We hypothesize this is because these lines are not in the NOD background. In the one case where we are aware that the DQ8 transgene/IA$_\beta$ knockout is being crossed onto the NOD, it may be that the breeding is not sufficiently far along to see the myocarditis phenotype (25). Alternately it is possible that the myocarditis seen in our line is caused by a founder effect; this question will be resolved by further breeding of existing DQ8 lines and/or by generation of additional new lines in the NOD background. The importance of the NOD background in contributing to the autoimmune myocarditis phenotype seen in our DQ8 transgenic animals is also supported by results obtained with certain other NOD MHC congenic lines. Although the introduction of non-IA^{g7} MHC alleles onto the NOD background frequently confers protection from diabetes, in some of these lines enhanced spontaneous autoimmune infiltration of organs other than islets has been observed. For example, NOD.H2^{h4}(IA^k) mice were found to develop spontaneous destructive infiltration of the thyroid at a rate much higher than NOD, and when sodium iodide was added to the drinking water, thyroid lesions were seen in ≈60% of the NOD.H2^{h4} mice, whereas dietary iodine had no effect on thyroiditis rates in NOD animals (26, 27). If it does turn out that a variety of non-MHC loci on the NOD background confer susceptibility to autoimmune myocarditis in $DQ8^{+/+},IA_\beta^{-/-}$ animals, it will be of interest to see whether these loci are similar or identical to the *Idd* loci, which confer susceptibility to autoimmune diabetes in the WT NODs (28).

Cardiac myosin is the most abundant cardiomyocyte-specific antigen; it accounts for a significant fraction of the mass of the heart and is frequently targeted by the immune system in other myocarditis models (29–31). It is interesting that in both our DQ8 NOD model and in many humans with IDCM (32, 33), autoantibodies against cardiac myosin occur. We were able to show moderate T cell proliferative responses to this antigen as well. However, whether or not cardiac myosin represents a key initiating autoantigen in the $DQ8^{+/+},IA_\beta^{-/-}$ NOD model remains to be proven. It could be that its sheer abundance and the phenomenon of intermolecular epitope spreading cause the autoimmune response to rapidly generalize from other much less abundant tissue-specific antigens. If this is indeed true, then it is likely that the inciting antigens in the $DQ8^{+/+},IA_\beta^{-/-}$ NOD model generate peptides capable of binding DQ8, and the model holds the potential for one day discovering the nature of these epitopes.

Given the immunological nature of the acute or chronic myocarditis leading to IDCM in humans, it would seem likely that certain HLA haplotypes might be associated with the condition. A number of studies have found an association with

DR4 (34–37), although this finding was certainly not universal (38–40). A lesser number of HLA-association studies included DQ typing (41–44), and considered together these fail to reach any consensus about the nature of susceptibility alleles. However, given the possibility that DR4 may sometimes be associated, because DR4 is in linkage disequilibrium with DQ8, it may be that in the affected DR4 individuals it is actually the DQ8 molecule that plays a major role in disease initiation and/or progression. Perhaps under certain environmental stresses the DQ8 molecule is predisposed to bind and present some key cardiomyocyte-specific epitope that initiates disease. In this way the DQ molecule would dictate the "choice" of the cell type or organ targeted by the autoimmune process. However in the present study, a single founder line has been investigated. The idea that DQ8 is a key factor in targeting cardiomyocytes for autoimmunity would require the same result in several more independent founder lines. Nevertheless, the $DQ8^{+/+},IA_\beta^{-/-}$ NOD line presented here provides a very useful animal model for cardiac scientists studying chronic, progressive inflammation of the heart muscle and the effects of this on both the conduction system and pumping functions of the heart. Thus, the model should be useful for investigating the etiology of IDCM and to test possible new therapies. Because the progression of the autoimmune inflammatory process in the heart can be followed over time by using noninvasive but highly sensitive ECG measurements, the model should also be useful more generally for testing new therapies directed against any spontaneously arising, organ-specific, cell-mediated autoimmune process.

1. Dec, G. W. & DeSanctis, R. W. (1998) in *Scientific American Medicine*, eds. Dale, D. C. & Federman, D. D. (Scientific American, New York), pp. XIV–1.
2. Manolio, T. A., Baughman, K. L., Rodeheffer, R., Pearson, T. A., Bristow, J. D., Michels, V. V., Abelmann, W. H. & Harlan, W. R. (1992) *Am. J. Cardiol.* **69,** 1458–1466.
3. Hosenpud, J. D. & Jarcho, J. A. (2000) in *Congestive Heart Failure*, eds. Hosenput, J. D. & Greenberg, B. H. (Lippincott, Philadelphia), pp. 281–284.
4. Brown, C. A. & O'Connell, J. B. (1995) *Am. J. Med.* **99,** 309–314.
5. Cetta, F. & Michels, V. V. (1995) *Ann. Med.* **27,** 169–173.
6. Liu, J., Purdy, L. E., Rabinovitch, S., Jevnikar, A. M. & Elliott, J. F. (1999) *Diabetes* **48,** 469–477.
7. Michelakis, E. D., Weir, E. K., Bateson, J., Waite, R., Kyoto, H. & Archer, S. L. (2001) *Am. J. Physiol.* **280,** L1138–L1147.
8. Pummerer, C. L., Luze, K., Grassl, G., Bachmaier, K., Offner, F., Burrell, S. K., Lenz, D. M., Zamborelli, T. J., Penninger, J. M. & Neu, N. (1996) *J. Clin. Invest.* **97,** 2057–2062.
9. Bachmaier, K., Neu, N., de la Maza, L. M., Pal, S., Hessel, A. & Penninger, J. M. (1999) *Science* **283,** 1335–1339.
10. Sadelain, M. W., Qin, H.-Y., Lauzon, J. & Singh, B. (1990) *Diabetes* **39,** 583–589.
11. Penninger, J. M., Pummerer, C., Liu, P., Neu, N. & Bachmaier, K. (1997) *APMIS* **105,** 1–13.
12. Neumann, D. A., Lane, J. R., Wulff, S. M., Allen, G. S., LaFond-Walker, A., Herskowitz, A. & Rose, N. R. (1992) *J. Immunol.* **148,** 3806–3813.
13. Bachmaier, K., Neu, N., Yeung, R. S., Mak, T. W., Liu, P. & Penninger, J. M. (1999) *Circulation* **99,** 1885–1891.
14. Bryant, D., Becker, L., Richardson, J., Shelton, J., Franco, F., Peshock, R., Thompson, M. & Giroir, B. (1998) *Circulation* **97,** 1375–1381.
15. Kubota, T., McTiernan, C. F., Frye, C. S., Slawson, S. E., Lemster, B. H., Koretsky, A. P., Demetris, A. J. & Feldman, A. M. (1997) *Circ. Res.* **81,** 627–635.
16. Kubota, T., McTiernan, C. F., Frye, C. S., Demetris, A. J. & Feldman, A. M. (1997) *J. Cardiac Failure* 117–124.
17. Nishimura, H., Okazaki, T., Tanaka, Y., Nakatani, K., Hara, M., Matsumori, A., Sasayama, S., Mizoguchi, A., Hiai, H., Minato, N. & Honjo, T. (2001) *Science* **291,** 319–322.
18. Virmani, R., Burke, A., Farb, A. & Atkinson, J. B. (2001) in *Cardiovascular Pathology*, ed. Virmani, R. (Saunders, Philadelphia), Vol. 40, pp. 289–293.
19. Nabozny, G. H., Baisch, J. M., Cheng, S., Cosgrove, D., Griffiths, M. M., Luthra, H. S. & David, C. S. (1996) *J. Exp. Med.* **183,** 27–37.
20. Abraham, R. S., Kudva, Y. C., Wilson, S. B., Strominger, J. L. & David, C. S. (2000) *Diabetes* **49,** 548–554.
21. Kudva, Y. C., Deng, Y. J., Govindarajan, R., Abraham, R. S., Marietta, E. V., Notkins, A. L. & David, C. S. (2001) *Hum. Immunol.* **62,** 1099–1105.
22. Wen, L., Wong, F. S., Sherwin, R. & Mora, C. (2002) *J. Immunol.* **168,** 3635–3640.
23. Wen, L., Wong, F. S., Burkly, L., Altieri, M., Mamalaki, C., Kioussis, D., Flavell, R. A. & Sherwin, R. S. (1998) *J. Clin. Invest.* **102,** 947–957.
24. Wen, L., Chen, N. Y., Tang, J., Sherwin, R. & Wong, F. S. (2001) *J. Clin. Invest.* **107,** 871–880.
25. Kudva, Y. C., Rajagopalan, G., Raju, R., Abraham, R. S., Smart, M., Hanson, J. & David, C. S. (2002) *Hum. Immunol.* **63,** 987–999.
26. Wicker, L. S., Todd, J. A. & Peterson, L. B. (1995) *Annu. Rev. Immunol.* **13,** 179–200.
27. Rasooly, L., Burek, C. L. & Rose, N. R. (1996) *Clin. Immunol. Immunopathol.* **81,** 287–292.
28. Vyse, T. J. & Todd, J. A. (1996) *Cell* **85,** 311–318.
29. Rose, N. R., Beisel, K. W., Herskowitz, A., Neu, N., Wolfgram, L. J., Alvarez, F. L., Traystman, M. D. & Craig, S. W. (1987) *Ciba Found. Symp.* **129,** 3–24.
30. Afanasyeva, M., Wang, Y., Kaya, Z., Park, S., Zilliox, M. J., Schofield, B. H., Hill, S. L. & Rose, N. R. (2001) *Am. J. Pathol.* **159,** 193–203.
31. Rose, N. R. & Hill, S. L. (1996) *Clin. Immunol. Immunopathol.* **80,** S92–S99.
32. Caforio, A. L., Goldman, J. H., Haven, A. J., Baig, K. M. & McKenna, W. J. (1996) *Int. J. Cardiol.* **54,** 157–163.
33. Lauer, B., Schannwell, M., Kuhl, U., Strauer, B. E. & Schultheiss, H. P. (2000) *J. Am. Coll. Cardiol.* **35,** 11–18.
34. Carlquist, J. F., Menlove, R. L., Murray, M. B., O'Connell, J. B. & Anderson, J. L. (1991) *Circulation* **83,** 515–522.
35. Anderson, J. L., Carlquist, J. F., Lutz, J. R., DeWitt, C. W. & Hammond, E. H. (1984) *Am. J. Cardiol.* **53,** 1326–1330.
36. Martinetti, M., Dugoujon, J. M., Caforio, A. L., Schwarz, G., Gavazzi, A., Graziano, G., Arbustini, E., Lorini, R., McKenna, W. J., Bottazzo, G. F., *et al.* (1992) *Hum. Immunol.* **35,** 193–199.
37. Limas, C. J. (1996) *Int. J. Cardiol.* **54,** 113–116.
38. Hiroi, S., Harada, H., Nishi, H., Satoh, M., Nagai, R. & Kimura, A. (1999) *Biochem. Biophys. Res. Commun.* **261,** 332–339.
39. Harcombe, A. A., Sharples, L., Large, S. R., Wallwork, J., Weissberg, P. L. & Joysey, V. (1999) *Int. J. Cardiol.* **68,** 31–37.
40. Lozano, M. D., Rubocki, R. J., Wilson, J. E., McManus, B. M. & Wisecarver, J. L. (1997) *J. Cardiac Failure* **3,** 97–103.
41. Osa, A., Almenar, L., Palencia, M., Puig, N., Chirivella, M. & Montoro, J. (1999) *Clin. Cardiol.* **22,** 292–296.
42. Carlquist, J. F., Ward, R. H., Husebye, D., Feolo, M. & Anderson, J. L. (1994) *Am. J. Cardiol.* **74,** 918–920.
43. Limas, C. J., Limas, C., Goldenberg, I. F. & Blair, R. (1995) *Am. Heart J.* **129,** 1141–1144.
44. Luppi, P., Alexander, A., Bertera, S., Noonan, K. & Trucco, M. (1999) *J. Biol. Regul. Homeostatic Agents* **13,** 14–26.